Biomethane recovery performance and microbial community dynamics of a high-biomass submerged AnMBR (HBSAnMBR) treating abattoir wastewater

Biomethane recovery performance and microbial community dynamics of a high-biomass submerged AnMBR (HBSAnMBR) treating abattoir wastewater

Rajneesh Kumar Gautam [a], Nuwan Vithanage [b], Nandkishor More [c], Shobha Muthukumaran [a], Dimuth Navaratna [a,d,*]

[a] Institute for Sustainable Industries & Liveable Cities, College of Sport, Health and Engineering, Victoria University, Melbourne, VIC 3011, Australia
[b] Agriculture and Food Division, Commonwealth Scientific and Industrial Research Organization (CSIRO), Melbourne, VIC 3030, Australia
[c] School of Earth and Environmental Science, Department of Environmental Science, Babasaheb Bhimrao Ambedkar University, Lucknow 226025, India
[d] ITCGU, Faculty of Engineering, University of Peradeniya, Prof. E. O. E. Pereira Mawatha, Kandy 20000, Sri Lanka

ARTICLE INFO

ABSTRACT

This study investigated the treatment and biomethane recovery performance of a high-biomass submerged anaerobic membrane bioreactor (HBSAnMBR) treating abattoir wastewater in six operational phases (Phases 1 – 6) at an organic loading rate (OLR) range of 1.05 – 7 kg-COD/m^3/d. The HBSAnMBR system demonstrated a biomethane recovery of 75.5 $\pm$ 2.0% and COD removal efficiency of 98.8 $\pm$ 0.71% during the most sustainable operational phase at an OLR of 4 kg-COD/m^3/d. Volatile fatty acids (VFAs) such as acetic, propanoic, isobutyric, and valeric acids significantly correlated with OLR and biomethane production, while butyric and isovaleric acid concentrations were unaffected. The biomethane recovery performance of the HBSAnMBR system correlated positively with microbial community dynamics in different operational phases. The functional analysis of the microbiome indicated that *Pseudomonas* and *Anaerolineaceae* played a significant role in the hydrolysis and fermentation of complex organic matter, which led to the production of VFAs and other intermediate products. *Methanothrix* were observed to utilize acetate for acetoclastic methanogenesis at OLR 4 kg-COD/m^3/d, producing the highest biomethane. On the contrary, the acetoclastic methanogenesis was replaced by hydrogenotrophic methanogenesis by *Methanolinea* and *Methanospirillum at* OLR above OLR 4 kg-COD/m^3/d, leading to a decline in biomethane production.

1. Introduction

Abattoirs are one of Australia's largest high-organic wastewater producing industries, generating a discharge volume of 400,000 - 500,000 L/d from small to medium-sized abattoirs and more than 1 million litres per day (MLD) in larger plants [1]. The wastewater generated from abattoirs consists of high organic content, suspended solids, and colloidal particles, including elevated levels of proteins, lipids, and carbohydrates [2]. Discharging untreated/partially treated abattoir wastewater into sewers or waterways can cause serious environmental and health risks, and it also can accumulate fats, oils, and grease (FOG) in sewer networks, causing depletion of dissolved oxygen, a rise in turbidity, floating scum, and sludge deposits, causing treatment

facility overhauling [3]. These challenges can be mitigated by reducing the organic compounds in the abattoir wastewater using an efficient anaerobic pretreatment technology [4].

The efficiency of an anaerobic pretreatment technology primarily depends on substrate characteristics, operational parameters and conditions, and the diversity of microbial communities [5]. The microbial communities and their composition play a significant role in biomethane production and treatment performance, depending primarily on factors such as substrate characteristics, pH, temperature, solids retention time (SRT), and hydraulic retention time (HRT) [6,7]. The substrate characteristics, such as the moisture content, pH, chemical composition and particle size, also affect biomethane production through methanogenesis [8,9]. A wide range of microbial communities are responsible for

the methanogenesis process during anaerobic treatment [10], including fermentative and syntrophic acetogenic bacteria and methanogenic archaea [11]. These microorganisms contribute to the degradation of complex molecules into simpler compounds during the fermentative, acidogenic, acetogenic, and methanogenic stages [12,13].

The effective pretreatment of abattoir wastewater is significantly challenging due to its complex composition of contaminants, high organic and solid content, and rapid pH fluctuation [14]. The high-rate anaerobic pretreatment (HRAPT) system has been proven to be a reliable solution for industrial wastewater pretreatment with numerous benefits, including high organic loading potential, biomethane recovery, and complete biomass retention [15]. A biological-membrane separation system such as a submerged anaerobic membrane bioreactor (SAnMBR) significantly advances HRAPT for treating industrial wastewater treatment [16,17] such as abattoirs containing a high salinity, elevated concentrations of suspended solids (SS), and the presence of complex organic compounds [18,19].

Several SAnMBR studies have been conducted recently to pretreat high-strength food industry wastewater, including those generated at confectioneries, wineries, piggeries and dairies [20–22], but only a few studies focused on treating abattoir wastewater [23,24]. Subsequently, a focus has been on investigating the performance of a high-biomass SAnMBR (HBSAnMBR) operated at excessively high biomass concentrations [25,26]. Of these recent SAnMBR studies, no compelling and indicative evidence has been reported to intricate the relationship between biomethane recovery performance and the microbiome as a majority of these studies primarily focused on filtration and membrane fouling performances only [27], while a systematic analysis of biomethane recovery and the associated microbiome is still lacking.

This study therefore significantly advances the existing literature on abattoir wastewater treatment by presenting a comprehensive analysis of microbial dynamics and their role in producing biomethane in an HBSAnMBR system ($18 \leq$ MLSS (g/L) ≤ 35) operated at an OLR range of ($1.05 - 7$ kg-COD/m^3/d). It distinguishes itself by exploring a unique combination of microbial communities, particularly highlighting the roles of *Anaerolineaceae*, *Pseudomonas extremaustralis*, and *Candidatus Cloacimonas*, which have not been reported in the existing literature. The research also provides detailed insights into the variations of these microbial populations across different operational phases, including their adaptation from acetoclastic to hydrogenotrophic methanogenesis in response to changes in organic loading rates. Additionally, this study collectively investigates the biomethane recovery and treatment performance of an HBSAnMBR system while treating abattoir wastewater. The findings will indicate the suitability of microbial consortium and sustainable operating conditions of a high-biomass SAnMBR system for optimal biomethane recovery and superior treatment performance.

2. Materials and methods

2.1. High-biomass SAnMBR setup

The lab-scale HBSAnMBR experimental setup consists of a water-jacketed, constantly stirred glass fermenter (bioreactor) tank with a 5 L hydraulic capacity, 3.5 L working volume, and 1.5 L headspace (Fig. 1). A BIOSTAT® automated controller (Applikon Bio Console ADI 1035) controlled feed flow, stirrer speed, and pH in the HBSAnMBR. A peristaltic pump (Masterflex 7518–00) connected to the BIOSTAT® drew abattoir wastewater from a 5 L PVC feed storage tank by taking
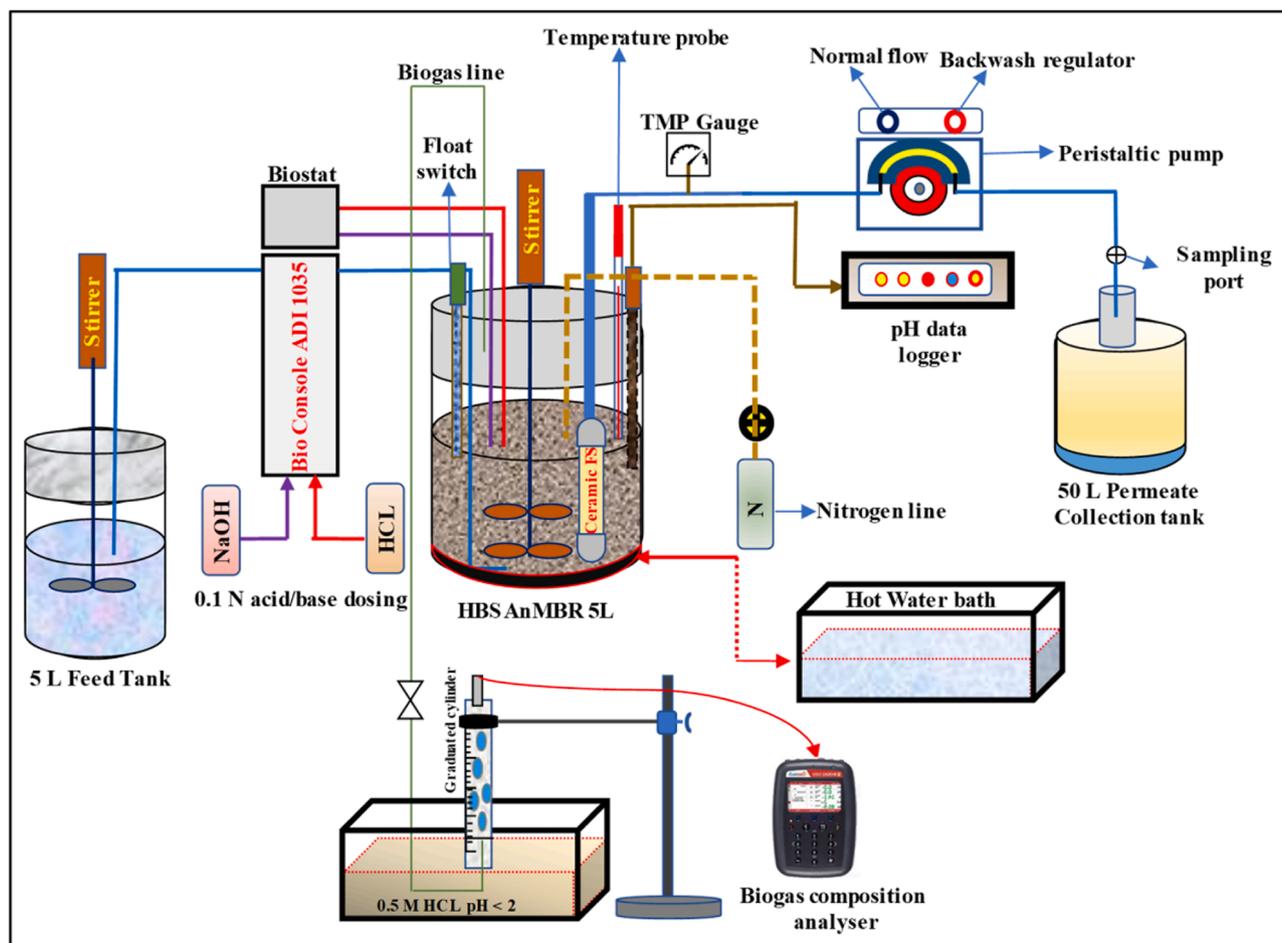
Fig. 1. A schematic representation of the HBSAnMBR setup used in this study.

signals from the electromechanical float switch suspended in the bioreactor. A peristaltic precision pump (Masterflex-L/s 07551–20) collected the HBSAnMBR-treated permeate in a 50 L PVC container. A nitrogen gas line and hot water bath attached to the HBSAnMBR maintained strict anaerobic and mesophilic (35 ± 2.5°C) conditions, respectively. A pH regulator system connected to the BIOSTAT® through a pH probe automatically maintained a neutral pH (7 ± 0.25) in the HBSAnMBR system by injecting 0.1 M HCl and 0.1 M NaOH via automatic dosing pumps. A mechanical stirrer was attached to the bioreactor to keep the inoculum in suspension. A flat-sheet (FS) ultra-filtration (UF) ceramic membrane module with an effective filtration area of $0.02 \ m^2$ was submerged in the bioreactor to separate biomass and generate high-quality treated effluent. A negative pressure gauge was attached to the membrane outlet via a peristaltic pump (Masterflex L/s 07551–20) to monitor transmembrane pressure (TMP). When the transmembrane pressure (TMP) reached 60 kPa during the investigation, ex-situ cleaning of the membrane was done following the manufacturer's (GuoChu Tech, Xiamen) protocol by immersing, bubbling, and backwashing the membrane with 3 g/L of NaClO. The membrane was then physically cleaned according to the protocol described by Navaratna and Jegatheesan [28].

2.2. HBSAnMBR experimental conditions and operation

The simulated abattoir wastewater for HBSAnMBR operation was prepared based on the real wastewater composition reported by [26] as per the recipe shown in Table S1 (supplementary information). The chemical compounds used to provide micronutrients and cations required for anaerobic digestion were added to a 5 L diluted sample, according to Table S1. The feed samples for a volume of 5 L were prepared and stored at 4 °C to prevent decay. The wastewater had a pH of 4.81 ± 1.5 and a COD of 8700 ± 250 mg/L. The pH of the feedstock was corrected to 7 ± 0.5 using 0.1 N NaOH and 0.1 N HCl before feeding the wastewater into the bioreactor. The bioreactor was occasionally purged (during chemical cleaning of the membrane module) with 0.5 L/min of nitrogen gas for 2 – 3 minutes to maintain strict anaerobic conditions. The bioreactor was operated at a controlled temperature of 35 °C, with a pH of 7 ± 0.25 and a stirring speed of 140 rpm. The inoculum was collected from an anaerobic digester located at the Gippsland Water Factory (GWF) in Victoria, Australia, having a mixed liquor suspended solids concentration (MLSS) of 65,850 mg/L and a mixed liquor volatile suspended solids concentration (MLVSS) of 57,209 mg/L. The HBSAnMBR was commissioned with three parts of substrate (feed) and seven parts of inoculum. The HBSAnMBR was operated continuously for 175 days in 6 distinct phases at OLR ranging from 1.05 to 7 kg-COD/m^3/d. These phases included acclimatization (Phase 1), transition (Phase 2), and stabilization (Phases 3, 4, 5, and 6). Due to an extremely high biomass concentration, Phase 1 was operated at an OLR of 1.05, 1.50, and 2.50 7 kg-COD/m^3/d to avoid membrane fouling. The OLR was increased in the subsequent phases by regulating the flow rate to achieve the designed values. The HBSAnMBR was operated in cycles of 30 min (two cycles/hr). Each cycle consisted of 25 min of filtration followed by 5 min of high-intensity backwashing. Since the key focus of this article is to investigate the biomethane recovery and treatment performance of an HBSAnMBR system, fouling performance was not evaluated and is beyond the scope of this study.

2.3. Analytical procedures

The physicochemical parameters such as COD and alkalinity were measured thrice weekly using standard colorimetric methods [29] using a DR 5000™ UV-Vis Spectrophotometer. The MLSS and MLVSS concentrations of the HBSAnMBR sludge samples were measured thrice a week using standard methods [29]. The concentration of Volatile fatty acids (VFA) was determined using gas chromatography (GC) (GC2010, Shimadzu), equipped with a flame ionization detector (FID) and a 30 m

x 0.25 mm×0.25 µm chromatographic column with nitrogen as a carrier gas. 2 µL of each sample was injected to the GC. The detector temperatures were set at 230 °C and 250 °C, respectively, with a split ratio of 30, a flow rate of 40 mL/min, and an N_2 partial pressure of 0.4 MPa. To determine the volume of biogas produced by the HBSAnMBR, a graduated cylinder was filled with 0.5 M HCl solution, inverted, and partially submerged in a container holding 0.5 M HCl solution (Fig. 1). Gases produced in the HBSAnMBR during the experiment were introduced into the cylinder's submerged portion, allowing the HCl solution to prevent the interference of gases collected. The collected gases displaced the HCl solution inside the cylinder, and the daily volume of produced biogas was measured. The graduated cylinder had an opening at the top connected to the gas analyzer using a Masterflex tube. The composition of gases, including biomethane, was measured using a high-end gas analyzer (Geotech-Biogas Sampler 5000), and the data obtained were logged and processed through a Microsoft Excel spreadsheet.

2.4. Microbial community analysis using whole genome sequence (WGS)

2.4.1. DNA extraction from HBSAnMBR sludge

For microbiological analysis, 50 mL of sludge samples were collected weekly to investigate the microbial diversities during acclimatization and stable operation of HBSAnMBR to evaluate and correlate the biomethane production with the microbial communities involved. Of these, sludge samples with identifications: Sample ID 5 (Phase 1), sample ID 113 (Phase 3) and sample ID 142 (Phase 5) were collected during commissioning, in which (sample ID 5) from the acclimatization phase and (sample IDs 113 and 142) from stable phases of HBSAnMBR, respectively, were used in extracting the DNA. The DNA of the samples was extracted using a DNeasy PowerMax® Soil Kit (QIAGEN Pty Ltd, Australia). The purity of the extracted DNA was evaluated using Nanodrop (DeNovix DS-11) using A260/230 nm and A260/280 nm (Life Sciences, Australia). DNA samples were kept at −20 °C until further analysis.

2.4.2. Whole genome sequencing (WGS) and bioinformatics analysis

The whole genome sequencing (WGS) of the extracted DNA samples was conducted by the Australian Genome Research Facility (AGRF, Melbourne, Australia). Library preparation was conducted using the Illumina DNA Preparation (M) kit on the Illumina NovaSeq 6000 platform with 150PE chemistry. The standard MetaWGS provided read-based classification analysis results. All MetaWGS sequencing samples have undergone quality control to assess the sequencing and library preparation quality. The bioinformatics pipeline consists of read quality control (FASTQC), reference strain determination (Mash), read mapping to the reference strain (BWA), de novo genome assembly (Spades), genome annotation (Prokka), phylogenetic analysis (PAML, Roary and RAxML) and functional analysis (HUMAnN2) [30,31]. Additionally, the raw read sequences were pre-processed and then processed using Kraken2 (version 2.0.8) and Bracken (version 2.5) for profiling the composition of microbial communities using a custom-built database using Qiime2 and an automated One Codex database. The database uses genomes from the National Centre for Biotechnology Information (NCBI) consisting of bacterial, fungal and viral sequences [32]. Human, plant and other vector sequences were also included in the database for quality control. Two pipelines were used to obtain metagenomic-based taxonomic profiling (Qiime 2 and One Codex). Functional profiles were generated using HUMAnN2 (version 2.8.1) with uniref90 and chocophlan as reference databases. Automatic annotations were validated manually for the genes involved in metabolic pathways of interest with the integrated MicroCyc and KEGG (Kyoto Encyclopedia of Genes and Genomes) databases [33].

2.5. Evaluation of cumulative biomethane production curves using kinetic modelling

During Phases 1–6, the cumulative biomethane yield was simulated and assessed using the modified Gompertz model (Eq. 1). The Gompertz model was specifically used in this study due to its accuracy and reliability in predicting biomethane production, as reported in several SAnMBR studies [34,35].

The modified Gompertz model equation [36] is expressed as:

$$y = P * \exp\left\{ -\exp\left[R * \frac{e}{P} * (L - t) + 1 \right] \right\} \tag{1}$$

Where y represents cumulative biomethane production (L-CH$_4$/g-COD) at a given time (d), P refers to maximum biomethane production potential (L-CH$_4$/g-COD), R refers to maximum biomethane production rate (L-CH$_4$/g-COD/d), L is the lag phase time (d), and e is Euler's constant equal to 2.718282 [36]. Parameters P, R, and L were calculated using a minimum residual sum of squares at a 95% confidence interval (CI) [37]. The best results for curve fitting correspond to a higher correlation coefficient value (R^2). A paired sample t-test was conducted on the findings of the fitting obtained from the modified Gompertz model. In addition, a variance analysis (ANOVA) was conducted in SPSS v.28 to validate the fitting results.

3. Results and discussion

3.1. Influence of organic loading rate (OLR) on biomass concentration in a high-biomass SAnMBR (HBSAnMBR)

Organic loading rate (OLR) and biomass concentration are essential parameters for the filterability and operational stability of a SAnMBR system. During commissioning (Phase 1, 0 – 15 d), the mixed liquor of the HBSAnMBR system was in a semi-solid state due to its extremely high biomass (MLSS) concentration averaging 34.34 g/L. Due to this, the OLR was purposefully kept low at 1.05 kg-COD/m^3/d, leading to a low biomass yield of 0.13 g-MLSS/g-COD. However, a high decay rate of

biomass (k$_{dx}$) of 0.06/d was observed during this period at F/M of 0.08 g-COD/g-MLSS, as shown in Table 1. This could be attributed to a lack of food availability, causing substantial cell decay due to endogenous respiration [38]. The OLR was further increased to 1.5 kg-COD/m^3/d and 2.5 kg-COD/m^3/d after 15 and 65 days of operation, respectively (Phase 1). The biomass concentration during this period was recorded as 21.14 and 18.72 g/L range, respectively. Due to the relative increase in OLR (2.5 kg-COD/m^3/d) towards the end of Phase 1 (45 – 65 d), the F/M ratio and biomass yield (Y) increased to 0.12 g-COD/g-MLSS and 0.15 g-MLSS/g-COD, respectively. In contrast, due to the availability of sufficient food, the decay rate of biomass (k$_{dx}$) decreased by 33% from 0.06/d (0 – 15 d) to 0.04/d (46 – 65 d), indicating effective acclimatization.

During Phase 2, there was a 25% increase in F/M due to an increase in OLR (3.5 kg-COD/m^3/d), leading to a higher biomass concentration and yield (Y), averaging at 24.30 g/L and 0.31 g-MLSS/g-COD, respectively, as shown in Table 1. A low decay rate of biomass (k$_{dx}$) during this period indicates that the microorganisms utilized sufficient organic matter in the system for their assimilation, implying that Phase 2 was a transition towards stabilization of the HBSAnMBR system. This observation agreed with previous studies that reported a positive correlation between biomass yield and OLR in an SAnMBR system [39,40]. Despite a high OLR (4 kg-COD/m^3/d) and F/M (0.19 g-MLSS/g-COD) in Phase 3, the MLSS concentration stabilized around 20 g/L, correlating positively with biomass yield (0.18 g-COD/g-MLSS) indicating that HBSAnMBR reached a stable condition. The decay rate of biomass (k$_{dx}$) was recorded as the lowest (0.02/d) during this period, showing a steady-state condition for the microorganisms [41]. A high F/M ratio during the steady state indicates the beginning of increasing microbial dominance [42, 43]. Suppose the substrate is continuously fed to the system at a higher rate. In that case, it can lead to substrate overloading and process instability [42].

As the OLR was increased in subsequent phases (Phases 4, 5, and 6), a low fluctuation in biomass concentration was observed. However, it should be that despite high OLR during these phases, the F/M decreased and stabilized around 0.16 g-MLSS/g-COD, with a high decay rate (k$_{dx}$),

Table 1
Performance of HBSAnMBR during different operational phases.

Phase		Phase 1			Phase 2	Phase 3	Phase 4	Phase 5	Phase 6
Days of Operation	d	0–15	16–45	46–65	66–84	85–110	111–125	126–150	151–175
OLR	(kg-COD/m^3/d)	1.05	1.50	2.50	3.50	4.00	5.00	6.00	7.00
HRT	h	80.4	52.56	31.2	22.8	19.2	15.6	13.2	11.04
F/M	g-COD/g-MLSS	0.08 ± 0.02	0.13 ± 0.03	0.12 ± 0.009	0.15 ± 0.02	0.19 ± 0.01	0.16 ± 0.011	0.17 ± 0.008	0.16 ± 0.01
Y	g-MLSS/g-COD	0.13	0.12	0.15	0.31	0.18	0.23	0.25	0.25
K$_{dx}$	1/d	0.06	0.04	0.04	0.03	0.02	0.04	0.06	0.05
Parameters in the reactor (average)									
pH	-	7.21 ± 0.16	7.28 ± 0.14	7.21 ± 0.09	7.35 ± 0.10	7.02 ± 0.08	7.12 ± 0.09	7.22 ± 0.12	7.12 ± 0.15
Alkalinity	mg-CaCO$_3$/L	720.4 ± 95.47	915.5 ± 49.5	689.6 ± 64.2	1062.25 ± 58.3	1160.625 ± 114.7	1151 ± 73.14	1389.8 ± 102.6	1496.1 ± 73.3
MLSS	g/L	34.34 ± 3.42	21.14 ± 2.45	18.72 ± 1.73	24.30 ± 1.42	20.82 ± 1.03	19.30 ± 2.13	19.90 ± 3.14	22.09 ± 2.73
VFA$_T$	mg/L	424.9 ± 26	434.5 ± 32.4	395.3 ± 18.7	436.5 ± 38.5	437.5 ± 25.4	425.3 ± 16	450.3 ± 15.4	477.3 ± 16.9
Biomethane production									
Biomethane production rate	L-CH$_4$/d	0.16 ± 0.4	3.77 ± 1.07	4.12 ± 0.48	6.39 ± 0.63	8.43 ± 0.51	7.63 ± 0.65	7.31 ± 0.31	7.34 ± 0.15
Biomethane yield	L-CH$_4$/g-COD	0.02 ± 0.04	0.40 ± 0.08	0.43 ± 0.02	0.42 ± 0.02	0.48 ± 0.01	0.45 ± 0.01	0.44 ± 0.01	0.44 ± 0.01
composition	%	ND	68.7 ± 3.4	68.8 ± 0.4	67.9 ± 3.5	75.5 ± 2.0	74.1 ± 2.9	72.4 ± 0.8	71.1 ± 1.2
Removal Efficiency									
COD	%	81.8 ± 2.29	84.3 ± 1.52	84.8 ± 0.98	90.0 ± 2.25	98.8 ± 0.71	95.7 ± 1.87	96.3 ± 0.39	94.41 ± 1.21

*ND- Not detected

as shown in Table 1, implicating increased toxicity in the bioreactor leading to significant death of microorganisms (k_{dx}) [44]. The increased toxicity leading to high decay rates (k_{dx}) could be attributed to high concentrations of butyric and isovaleric acids [45] during Phases 4, 5, and 6. In summary, the OLR and biomass concentration correlated positively with biomass yield (Y); however, high OLRs (above 4 kg-COD/m^3/d) resulted in significant death of microorganisms (k_{dx}) due to induced toxicity in the bioreactor.

3.2. Long-term treatment performance of the high-biomass SAnMBR (HBSAnMBR) system

The treatment performance of the HBSAnMBR was evaluated in terms of COD removal efficiency in six phases (Phases 1 – 6) during its 175 days of operations, as shown in Fig. 2a, Figure S1 (supplementary information), and Table 1. The F/M showed a positive correlation with the applied OLR but a negative correlation with the HRT, as shown in Fig. 2b. Increasing the OLR decreased the hydraulic retention time (HRT) from 80 to 11 d during Phases 1 – 6, respectively (Fig. 2b). The HBSAnMBR exhibited poor performance in terms of COD removal efficiency (81.8 ± 2.29, 84.3 ± 1.52, 84.8 ± 0.98%) during the acclimatization period (Phase 1) at OLR of 1.05, 1.5, and 2.5 kg-COD/m^3/d, respectively as shown in Fig. 2a, Figure S1, and Table 1. As the OLR was increased to 3.5 kg-COD/m^3/d in the subsequent phase (Phase 2), the COD removal efficiency increased to 90.0 ± 2.25%, showing a positive correlation with increasing OLR and decreasing HRT. With a decreased HRT (19.2 d) and increased OLR of 4 kg-COD/m^3/d in Phase 3, the HBSAnMBR demonstrated the highest COD removal efficiency (98.8 ± 0.71%) compared to other phases, as shown in Fig. 2a and Figure S1. However, as the OLR was increased to 5, 6, and 7 kg-COD/m^3/d in subsequent phases (Phases 4, 5, and 6), the COD removal efficiency of the HBSAnMBR showed a decreasing trend as shown in Fig. 2a and Table 1. This observation agreed with prior SAnMBR studies conducted under high-biomass conditions [46,47] at an OLR range of 0.8 – 4.7 kg-COD/m^3/d. Ideally, a higher OLR is reported as suitable for higher yield in terms of COD removal [48,49]. However, the reactor may be under stress in Phases 4 – 6 due to its high organic load, suggesting that high OLRs can have complex and varied impacts on the COD removal efficiency of the system [50]. Previous studies using the SAnMBR system observed high organic removal at high OLR under high-biomass conditions [51]. This study followed a similar performance, as shown in Fig. 2a, demonstrating an increasing trend of COD removal efficiency at increasing OLR during Phases 1 – 3, as shown in Fig. 2a. This indicates that a critical OLR exists beyond which the organic removal performance of an SAnMBR decreases under high-biomass conditions due to increased toxicity due to the significant death of microorganisms (k_{dx}), leading to the deficiency and inability of microorganisms to metabolize organic matter completely.

Fig. 2b shows the relation between HRT, F/M and the OLR. Specifically, a 10% reduction in HRT led to an approximate 25% increase in the F/M ratio, indicating an increased concentration of organics available to the microorganisms [52]. This indicates that a shorter HRT provides limited time for microorganisms to metabolize the organic matter, potentially leading to a decreased COD removal efficiency (Fig. 2a, Table 1), as observed during Phases 4, 5, and 6. Conversely, an increase in HRT correlated with a decrease in OLR, as shown in Fig. 2b. This suggests that the system is being fed a lower concentration of organics (Phases 1 and 2) over an extended period (0 – 84 d), potentially decreasing the metabolic pressure on the microbial communities. However, while this longer HRT ensures more thorough substrate utilization, it could also increase the risk of an increase in biomass and potentially lead to an accumulation of intermediate products such as VFAs [47]. In summary, In the present study, the HBSAnBR system achieved over 98% COD removal at an OLR of 4 kg-COD/m^3/d and was deemed sustainable for treating abattoir wastewater.

3.3. The concentration of volatile fatty acids (VFAs) during long-term HBSAnMBR operation

Fig. 3a illustrates the variation of volatile fatty acids (VFAs) with time. At the same time, the data points represent the time-based values during the HBSAnMBR operation. According to the findings of this study, the OLR correlated positively with the production of total volatile fatty acids (VFA$_T$) at higher OLR (Phases 3 – 7), as shown in Table 1, which resulted in a more efficient synthesis of VFA$_T$. It was also found that individual VFAs such as acetic, propanoic, isobutyric, and valeric acids significantly correlated with OLR. However, the concentrations of butyric and isovaleric acids remained relatively constant throughout the study, as shown in Fig. 3a. This suggests that a high OLR may only stimulate the synthesis of specific VFAs, such as acetates. This could be due to abattoir wastewater composition, as the production of VFA also depends on the substrate characteristics and the biochemical mechanism involved in its treatment [53,54].

In anaerobic wastewater treatment, acetic acid and butyric acid are the primary precursors to biogas production. Particularly, acetic acid has the most significant potential for biomethane recovery compared to other VFAs [55]. As shown in Fig. 3a, till day 85 (Phases 1 and 2), the VFAs with the highest concentrations were acetic acid (102.88 mg/L) and propanoic acid (145.24 mg/L), while the VFA with the lowest concentration was butyric acid (0 mg/L till day 18). Past studies [45,56] show that individual VFAs considerably influence biomethane generation. The metabolic degradation of acetic acid by methanogens increases biomethane generation [56]. On the contrary, butyric acid and its derivatives, on the other hand, inhibit biomethane production, resulting in a decreased biomethane recovery.

During the most sustained phase (Phase 3), operated at OLR 4 kg-COD/m^3/d, the acetic acid concentration was as high as 85.7 mg/L (Fig. 3a). In contrast, other VFAs such as propionic (58.5 mg/L), isobutyric (65.4 mg/L), butyric (72.6 mg/L), iso valeric (79.1 mg/L), and valeric (79.1 mg/L) acids were slightly lower than acetic acid during this phase (Fig. 3a). Comparatively, acetic acid had the highest concentration during the stable operation of HBSAnMBR (Phases 3 – 6), as shown in Fig. 3a. This observation could be related to acetoclastic methanogenesis, the major pathway for producing biomethane production during stable operation [57]. The concentration of butyric acid was highest in Phase 6, recorded at 76.5 mg/L, as shown in Fig. 3a, which may be attributed to the increased hydrolysis of complex organic compounds and subsequent butyric acid production via acidogenesis [58], leading to toxicity in the bioreactor [45]. On the other hand, the propionic acid concentration showed an increasing trend at increasing OLRs in Phases 4, 5 and 6, as shown in Fig. 3a. High propionic acid concentrations could inhibit biomethane recovery, possibly due to its slow degradation [47].

High organic loading in SAnMBR systems can increase acidification and accumulation of VFA$_T$, increasing alkalinity and inhibiting methanogenesis [59]. In SAnMBR, alkalinity acts as a buffering system that stabilizes pH by absorbing acids and neutralizing bases, thereby supporting microbial activity and assisting in efficient biodegradation for high biomethane production [60,61]. This study observed a positive correlation between alkalinity and OLR (Fig. 3b). An increasing trend of alkalinity can be seen at various OLRs during different phases (Phase 1 – 6), as shown in Fig. 3b, with OLR 7 kg-COD/m^3/d, attributing to the highest alkalinity of 1496 mg/L. Overall, the OLR positively correlated with VFAs and alkalinity during various phases of HBSAnMBR operation. However, high OLR may only stimulate the synthesis of specific VFAs. The concentrations of butyric, isovaleric and valeric acids increased at OLR 5, 6, and 7 kg-COD/m^3/d as shown in Fig. 3a, which inhibited the biomethane recovery (Table 1) and induced toxicity in the bioreactor leading to a significant death of microorganisms (k_{dx}), ultimately affecting the treatment performance.
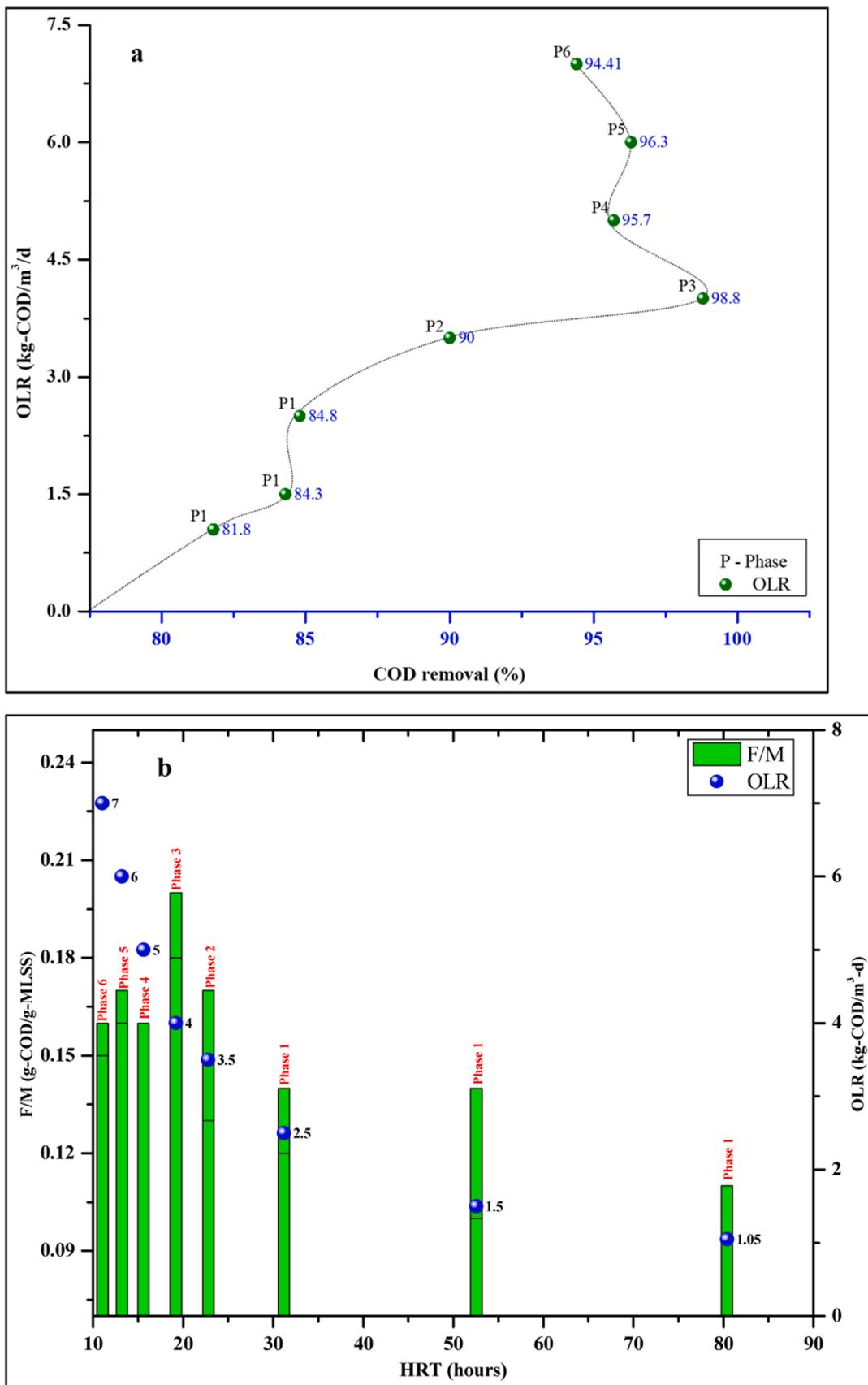
Fig. 2. Performance of the HBSAnBR treating abattoir wastewater: (a) COD removal efficiency at various OLRs; (b) Variation between F/M ratio and OLR vs. HRT.
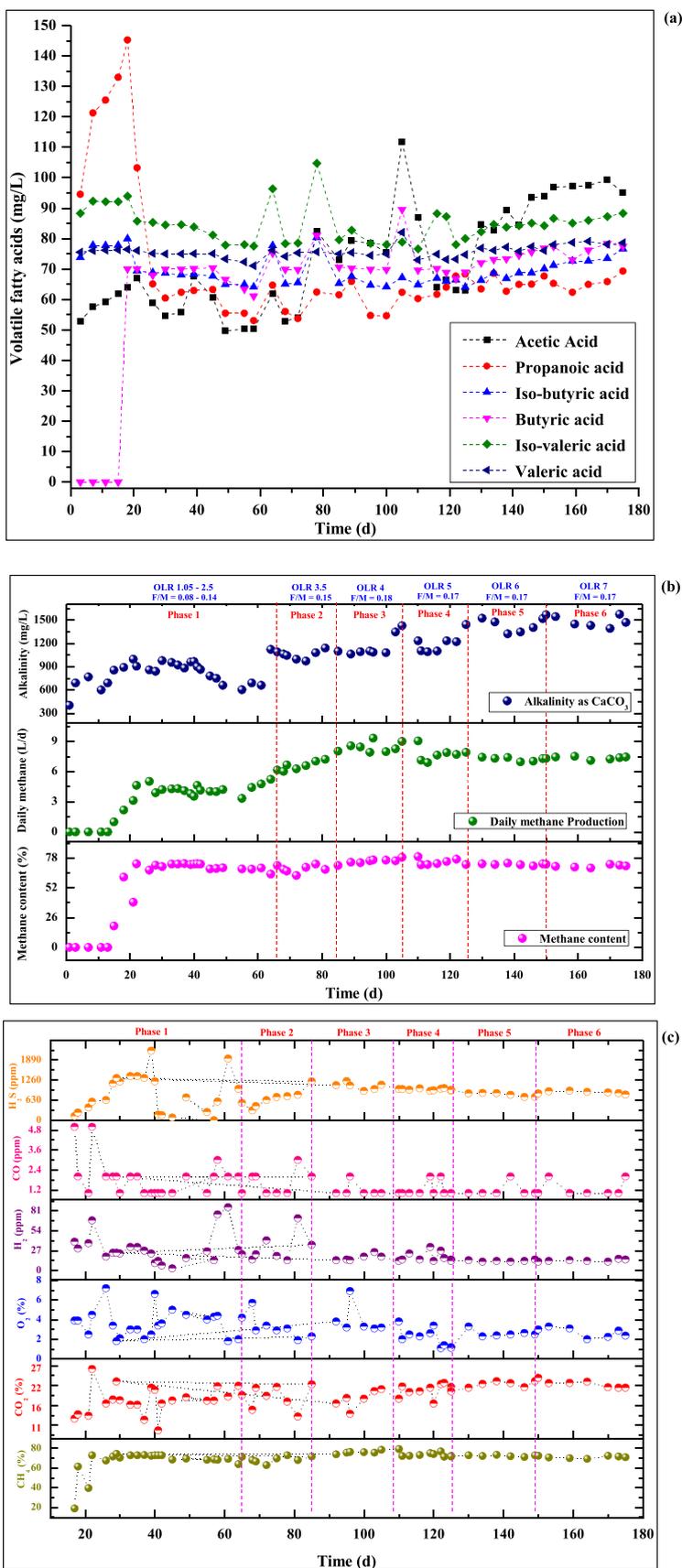
Fig. 3. Performance of HBSAnMBR during various phases in terms of; (a) Variation of volatile fatty acid concentration (mg/L); (b) Alkalinity (L/d), daily biomethane production (L/day) and methane concentration (%); (c) Variation of gaseous concentration in the produced biogas.

3.4. Biomethane recovery performance of HBSAnMBR

An average biomethane production rate of around 7.12 ± 0.25 L/d was recorded during this long-term study. The HBSAnMBR system started producing biogas from the 18th day of HBSAnMBR operation at an OLR of 1.5 kg-COD/m^3/d. The yield (L-CH$_4$/g-COD) and composition (%) of biomethane were recorded as the lowest during Phase 1 and 2, as shown in Table 1. A high and stable biomethane yield was recorded in Phases 3 – 6, with Phase 3 demonstrating the highest yield (0.48 ± 0.01 L-CH$_4$/g-COD) and biomethane concentration ($75.5 \pm 2.0\%$), as shown in Fig. 3b and Table 1. However, at OLR above 4 kg-COD/m^3/d (Phases 4, 5 and 6), the HBSAnMBR system started showing a decline in the production rate of biomethane as shown in Fig. 3b, suggesting high OLRs could impede the biomethane production rate due to high concentrations of individual VFAs such as butyric, propionic and iso-valeric acids [45,53], and reduced biodegradability of the substrate at higher OLRs [62].

Gases, including CO_2, O_2, H_2, and H_2S, were also produced during the HBSAnMBR operation, as shown in Fig. 3c. These gases could directly influence the biomethane production rate in an SAnMBR system [63]. Carbon dioxide (CO_2) concentrations were present in varying amounts throughout different phases of the experiment. An increasing CO_2 concentration (%) was observed in Phases 1 – 6, with the highest concentration observed during Phase 6 ($22 \pm 0.99\%$), as shown in Table 1. The changes in microbial populations and metabolic pathways may have contributed to the observed ascending variations in CO_2 concentration [64]. Traces of oxygen (1.1 – 7.2%) were identified in a few samples during Phases 1 and 2. This could be due to air leaks in the bioreactor or insufficient oxygen removal during feedstock pretreatment using nitrogen gas (N_2) purge. The hydrogen (H_2) concentration in biogas ranges from 3 to 86 parts per million (ppm), with the highest concentration measured on day 61 (Phase 1) at an OLR of 2.5 kg-COD/m^3/d, and the lowest concentration measured on day 142 (Phase 5), at an OLR of 6 kg-COD/m^3/d. This slight discrepancy in H_2 content may be attributable to a shift in the microbial community [65] during the acclimatization period (Phase 1) and toxicity induced at higher OLRs (Phases 5 and 6). Carbon monoxide (CO) concentration was found in the 1–5 ppm range during phases 1 – 6. Balat and Balat [66] reported that CO can be utilized as a substrate by certain microorganisms, including acetogenic bacteria, which can outcompete methanogens for the available carbon and energy sources. This leads to a shift in the microbial community and a decline in the population of methanogens, ultimately reducing biomethane production. However, at low concentrations (less than 50 ppm), CO has been shown to enhance biomethane production by providing a carbon source for acetoclastic methanogens. The hydrogen sulphide (H_2S) in the biogas was found in the range of 3.4–2186 ppm, with a maximum concentration of H_2S observed in Phase 1 (days 38 and 61) at an OLR of 2.5 kg-COD/m^3/d (Fig. 3c). During anaerobic treatment, the H_2S is primarily produced by sulphate-reducing bacteria (SRB). These bacteria use sulphate as an electron acceptor and organic compounds as electron donors to produce H_2S as a by-product. However, H_2S can inhibit the growth and activity of microorganisms, including methanogens, in the SAnMBR system [66]. Overall, the HBSAnMBR system demonstrated a consistent biomethane recovery. However, when OLRs exceeded 4 kg-COD/m^3/d, a reduction in biomethane production became evident, suggesting potential challenges associated with bioreactor toxicity and substrate biodegradability at elevated OLRs. Overall, the HBSAnMBR operation revealed the production of several gases and their influence on the biomethane production rate. Notably, CO_2, O_2, H_2, and H_2S concentrations varied significantly throughout the study, each having specific implications on biomethane recovery. These fluctuations were influenced by factors such as microbial population shifts, metabolic pathways, and operating conditions such as OLRs. Despite the consistent biomethane recovery observed in the HBSAnMBR system, elevated OLRs posed challenges, underscoring the need for optimal operational conditions to maintain efficient biomethane production.

3.5. Model simulation of biomethane production

Mathematical modelling was conducted using the modified Gompertz model to simulate the model parameters for predicting the biomethane production rates during different phases (Phase 1 – 6). The model simulated results fitted well with the experimental data, as shown in Fig. 4, and validated the experimental findings and trends of biomethane recovery across the HBSAnMBR operational phases. The modified Gompertz model demonstrated that the biomethane production potential (P) was highest for Phase 3 (12.11 L-CH$_4$/g-COD) and recorded lowest for Phase 1 (3.79 L-CH$_4$/g-COD). With increasing OLR in subsequent phases, there was a decline in biomethane production potential (P), as shown in Fig. 4. Other parameters, such as R (maximum biomethane production rate) and L (lag phase), positively correlated with the applied OLR and F/M. A statistical analysis using non-linear regression was conducted to find the correlation between model-simulated results and experimental data and found a correlation coefficient (R^2) (0.946 and 0.996) and p-value ($p < 0.05$) for Phases 1 – 6, as shown (Fig. 4, Table 2). The modified Gompertz model was found suitable to accurately predict model parameters and biomethane production rates in the HBSAnMBR system. From the modelling study and experimental investigation, OLR 4 kg-COD/m^3/d was found sustainable for recovering high-quality biomethane with a high yield of 0.48 L-CH$_4$/g-COD and production potential of 12.11 L-CH$_4$/g-COD. It can also be concluded that operating an HBSAnMBR system within a sustainable range of OLR is favourable for biomethane recovery and sustained operation.

3.6. Analysis of dynamics and composition of the microbiome in an HBSAnMBR system

Illumina sequencing yielded over 76.15 Gb reads with high-quality reads having an e-value cutoff of $10 - 5$ and a minimum alignment length of 50 bp. Samples were chosen and clustered into two main groups: acclimatization (Phase 1) and stable phases (Phases 3 and 5). Differences in microbial community diversity between HBSAnMBR operational stages were analyzed using phylogenetic distance metrics and visualized with a heatmap and principal component analysis (PCA) (Figures S2 (a) and (b)). Sample ID 5 (acclimatization), sample ID 113 and sample ID 142 (stable phases) contained 138,525,946 (29.85%), 150,996,310 (33.07%), and 138,525,946 (29.85%) high-quality reads, respectively. These were classified using One Codex. Microbiome features were characterized by comparing alpha and beta diversity and relative abundance. Alpha diversity of Bacteria, Eucaryota, Archaea and viruses was assessed using OTUs, Shannon (H') and Simpson (1-D) indexes. The sample representing the acclimatization phase (sample ID 5) showed higher diversity indexes than sample ID 113 and 142 (stable phases), indicating high microbial variability during the acclimatization phase of HBSAnMBR. In contrast, sample IDs 113 and 142 (stable phases) were less diverse, indicating domination by one or a few microbes. High microbial richness was observed to lead to improved anaerobic treatment [65].

The change in microbial diversity is attributed to changes in VFA concentration, alkalinity, and HRT during HBSAnMBR operation. Shifts in diversity among microbial communities were possibly due to transient species. Alpha and Beta diversity patterns were significantly correlated with functional differences between the microbial communities, similar to the alpha diversity patterns [67].

3.6.1. Taxonomic profiling of predominant microbes

In the HBSAnMBR sludge, Bacteria was the most dominant species, with populations of 76.99%, 63.53%, and 60.07% across Phases 1, 3, and 5, as illustrated in Fig. 5. The dominance of Bacteria in such systems can be attributed to their adaptability in different environmental
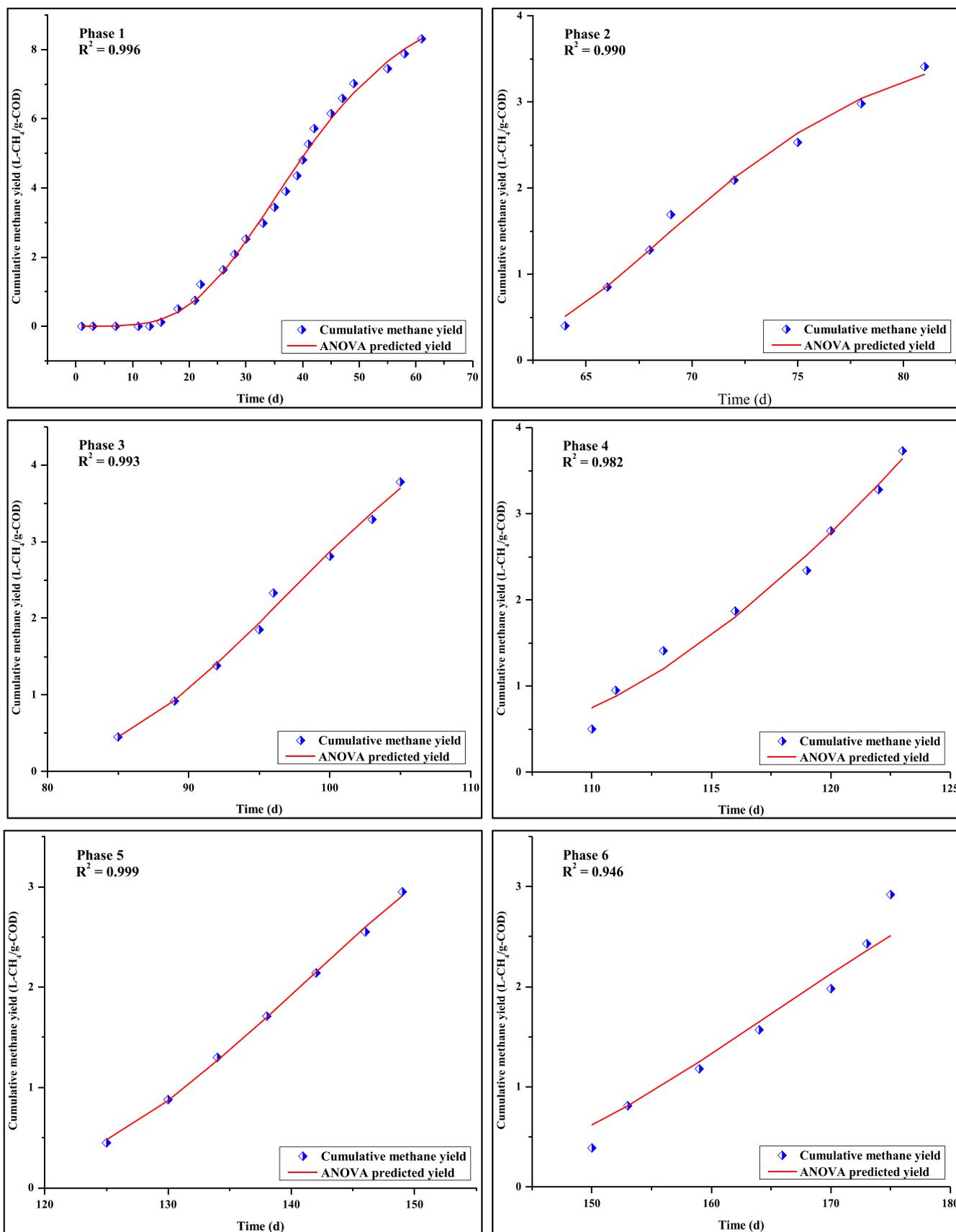
Fig. 4. Modified Gompertz model fitting results with experimental data for phases 1 – 6 at OLR 1.68, 3.50, 4, 5, 6 and 7 kg-COD/m^3/d.

Table 2
Kinetic parameters estimation for average cumulative methane production using the modified Gompertz model.

Phases	OLR	F/M	P	R	L	p-values	R^2	RSS
I	1.68*	0.11 ± 0.01	3.793	0.219	5.205	< 0.0001	0.996	0.035
II	3.50	0.13 ± 0.02	9.855	0.247	7.097	< 0.0001	0.990	0.015
III	4	0.19 ± 0.01	12.117	0.386	13.550	< 0.0001	0.993	0.014
IV	5	0.16 ± 0.01	11.928	0.318	14.689	<0.0001	0.982	0.032
V	6	0.17 ± 0.01	10.359	0.313	12.952	<0.0001	0.999	0.001
V1	7	0.16 ± 0.01	10.585	0.281	13.670	<0.001	0.946	0.065

* average OLR (kg-COD/m^3-d), F/M (g-COD/g-MLSS), P (L-CH4/g-COD) (biomethane production potential), R (L-CH4/g-COD/d) (Maximum biomethane production rate), L (d) (Lag phase), RSS- Residual sum of squares

Table 3
Alpha diversity indices of the microbiota during HBSAnMBR operation.

Sample ID	Phase	OTUs	Sympson	Shannon
5 (Acclimatization)	1	234	0.933	5.25
113 (Stable)	3	142	0.847	3.98
142 (Stable)	5	146	0.739	3.43

conditions, often outcompeting other microbial domains [68]. The presence of Archaea increased from an initial 6.7% in Phase 1–13.0% in Phase 5, which was found to be higher than in the previous study (< 4.7%) conducted by Matsubayashi, Shimada [12]. This increase can be attributed to the ability of certain Archaea to exploit specific niches in wastewater systems, particularly those rich in methane [69]. Fourteen dominant phyla, including *Chloroflexi*, *Pseudomonadota*, and *Actinobacteria*, exhibited variations in their proportions. This finding coincides with a previous study by Puengrang, Suraraksa [8]. The consistent abundance of *Anaerolineaceae* and their role in the breakdown of organic matter for biomethane production, highlights their critical role in anaerobic systems. Their presence correlates with VFA concentrations and biomethane composition in the HBSAnMBR system reported in previous sections (Sections 3.2 and 3.3).

During the acclimatization phase, microbes belonging to the *Pseudomonadota* phylum, notably *Pseudomonas extremaustralis* (11.9%), played a crucial role in metabolism. *P.extremaustralis* is a psychrotrophic and microaerophilic bacterium that exhibits remarkable stress resistance through the production of high levels of polyhydroxyalkanoates and gains redox potential, oxidative stress resistance, and biofilm formation under microaerophilic conditions [70]. The acclimatization phase also observed dominance from *Actinomycetales* and *Synergistaceae* microbes, known for their syntrophic metabolic activities in anaerobic environments [71]. *Actinomycetales*, known for their diverse metabolic capabilities, often play a crucial role in the degradation of complex organic compounds. In anaerobic environments, they might contribute to the initial breakdown of such compounds, making them available for other microbes in a syntrophic relationship [72].

On the contrary, *Synergistaceae* are known for their ability to degrade amino acids and other organic compounds under anaerobic conditions. They often participate in syntrophic associations, especially in environments where the breakdown of organic matter is a multi-step process that requires the collaboration of different microbial species. During the acclimatization phase in a bioreactor like the HBSAnMBR system, *Actinomycetales* and *Synergistaceae* might play pivotal roles in establishing a stable microbial community [71]. During the stable HBSAnMBR operation (Phases 3 and 5), a consistent microbiome consisting of *Anaerolineaceae, M. soehngenii,* and *Cloacimonetes* was observed [73]. The presence of *Cloacimonadota* in the HBSAnMBR system (previously known as *Cloacimonetes*) indicates its importance in decomposing complex organic matter [74].

Additionally, bacterial lineage relating to *Thermotogales* was found in sample IDs 113 and 142. These bacteria comprise anaerobic, mesophilic or thermophilic heterotrophs that possess the ability to ferment simple and complex sugars into H$_2$, CO$_2$, and acetate [75]. Moreover, the steady

phases (Phases 3 and 5) also contained *Verrucomicrobia,* a low abundant and phylogenetically divergent lineage degrading organic carbon. These microbes can be potentially novel bacteria and archaea with differential metabolic profiles, which must be explored in future studies.

3.6.2. Phylogenetic analysis and diversity of methanogens in the HBSAnMBR system

The microbiotas in sample IDs 5, 113, and 142 were categorized through the phylogenetic tree analysis. In these samples, 30, 25, and 18 distinct clusters were identified, respectively, with each cluster having a minimum of 20,000 reads, as shown in Figure S3(a), (b), and (c) (supplementary information). Within these clusters, the *Anaerolineaceae* cluster was observed along with *Levilinea, Leptolinea, Flexilinea,* and *Ornatilinea.* These microbes were present in all three samples, in varying concentrations, except for *Leptolinea*, which was only found in sample ID 142. *Anaerolineaceae* play a vital role in breaking down complex organic matter, thereby facilitating the initial stages of anaerobic digestion. Methanogenic archaea, including *Methanothrix* and *Methanosaeta*, were clustered together, with *Methanosaeta* having several partially classified isolates such as UBA70, UBA356, UBA332, UBA372, UBA458, and UBA286 (Figure S4 and S5(a and b)) which are are pivotal for biomethanogenesis. Additionally, *Methanospirillum* was observed in sample IDs 113 and 142, whereas *Candidatus Methanofastidiosum Methylthiophilus* was only found in sample ID 113. A notable cluster of *Bacteroidetes* was observed predominantly in sample ID 142 towards the end of the process. These microbes can be linked with the concentration of organic and inorganic compounds in the wastewater and reflected in the F/M ratio [76].

Regarding the diversity of methanogens, it was identified that Archaea play a vital role in the high-biomass SAnMBR system, especially during abattoir wastewater treatment. The archaeal populations in sample IDs 5, 113, and 142 were 6.69%, 13.02%, and 9.5%, respectively. These archaea belonged to 14 phyla, with *Euryarchaeota* being the most dominant, underscoring its critical involvement in methanogenesis. Methanogens, known for their ability to produce biomethane, play a critical role in biomethanogenesis. *Methanothrix soehngenii* was identified as the dominant Archaea in this population. This methanogen is primarily known for its role in acetoclastic methanogenesis converting acetate into biomethane and carbon dioxide [77]. The discovery of novel bacteria related to Methanosaeta, which follows a similar methanogenic pathway, further highlights the complexity and efficiency of the biomethanogenesis process in the system. During the analysis, several novel bacteria related to *Methanosaeta* were discovered. These bacteria were found to follow the acetoclastic methanogenesis pathway, releasing biomethane and carbon dioxide by decarboxylating acetate, but they cannot reduce carbon dioxide with hydrogen to produce biomethane or other methanogenic substrates (formate, methanol, methylamines) [78]. Along with *Methanothrix* and *Methanosaeta*, other dominating methanogenic genera, such as *Methanospirillum* and *Methanosarcina*, were identified in the HBSAnMBR system. The variation in concentrations of these key microbial groups across different samples and phases of the HBSAnMBR operation highlights the intricate syntrophic relationships essential for efficient biomethane production and wastewater treatment.
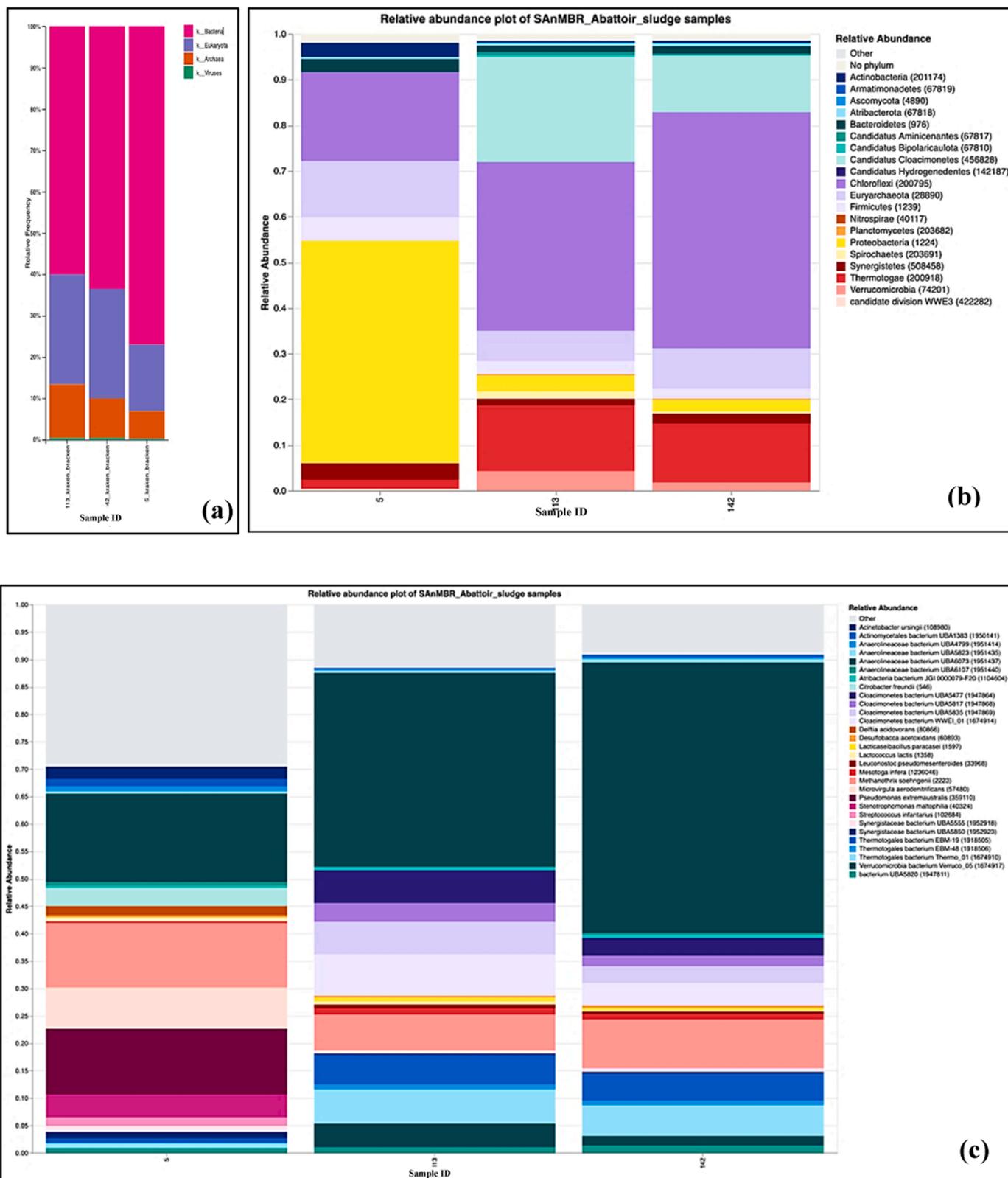
Fig. 5. Predominant microbiome genera isolated from HBSAnMBR during the different stages of operation at (a) Domain level, (b) Phylum level, and (c) Species level.

Hydrogenotrophic methanogens, including *Methanospirillum* and *Methanoculleus*, were also observed in the samples, as shown in Figures S4 and S5(b). These methanogens can reduce CO_2 to CH_4 with hydrogen as the primary electron donor and formate. However, their abundances were lower than the acetoclastic methanogens and

increased towards the end of the HBSAnMBR operation (Phase 5). The overall microbial diversity and relative abundance of methanogenic populations varied across different HBSAnMBR operational stages and significantly correlated with biomethane production. Their presence and activities underline the importance of understanding microbial

dynamics and methanogenic pathways for optimizing wastewater treatment processes and enhancing biomethane yield. The phylogenetic analysis (tree) and heat map further confirmed this variation, as shown in Figure S3 (a). These findings offer new insights into the syntrophic relationship between *Anaerolineaceae* and *Methanothrix* in a high-biomass SAnMBR system.

3.6.3. Functional analysis and biomethane production pathways in the HBSAnMBR system

Functional analysis of the metagenome was used to verify the roles of dominant microorganisms and their metabolic pathways. Most abundant pathway modules were related to carbohydrate and lipid metabolism, nucleotide and amino acid metabolism, carbon fixation, biomethane, sulphur, nitrogen and energy metabolism pathways (Figure S6). This study observed a high abundance of carbohydrate metabolisms, such as glycolysis/gluconeogenesis, pentose phosphate pathway, amino acid and nucleotide metabolisms and TCA cycle, as shown in Figure S6 (supplementary information), suggesting that HBSAnMBR microbiota were actively involved in the digestion of carbohydrates and energy conversion during its operation. This finding agreed with a previous study by Guo, Peng [71]. Serine, cysteine, arginine, and glycine metabolism were observed in good coverage, as shown in Figure S6. The high glycine cleavage pathway expression in this study indicates the activation of metabolic pathways for acetate metabolism. Conversely, nucleic acid metabolism, including pyrimidine and purine biosynthesis and salvage pathways, were prominent, highlighting the possibility of using them as a nitrogen and phosphorus source by microorganisms in biomethane production [79].

The components in the microbial biomethanogenesis pathways were identified as illustrated in Figure S6. Methyl coenzyme-M reductase enzyme among *Methanothrix* was found in high coverage, which is a critical enzyme responsible for the acetoclastic methanogenic pathway which catalyzes biomethane production by reducing the methyl group bound to coenzyme-M encoded by a gene (mcrA). Methyl coenzyme-M reductase, which directly converts acetate into biomethane and carbon dioxide, was found in Methanosaeta [80]. Thus, *Methanothrix* may be metabolically active via the carbon dioxide reduction pathway rather than the acetate decarboxylation pathway, yielding more energy [81]. While *Pseudomonas* degrade the organic compounds, the predominant *Anaerolineaceae* could be responsible for producing these intermediate metabolites (i.e., acetate, butyrate, isobutyrate, and propionate, particularly acetate. acetate) [82]. *Anaerolineaceae* possess acetyl-CoA synthetase, which converts acetyl-CoA to acetate or ethanol as fermentation by-products [81].

Furthermore, *Methanosaeta* can accept electrons via direct interspecies electron transfer (DIET) to reduce carbon dioxide to biomethane, where ethanol is the primary substrate [83]. This indicates that *Methanothrix* and *Methanosaeta* could remain in the system due to the role of *Anaerolineaceae* fatty acids transforming into acetate and likely engaging in syntrophic cooperation during HBSAnMBR operation [84]. Hydrogenotrophic methanogenesis pathways were also identified, especially in Phase 5; however, the abundance of genes encoding enzymes in the acetoclastic pathway was much higher than that involved in hydrogenotrophic and methylotrophic pathways [71].

A significant increase in *Anaerolineaceae* and *Pseudomonas* was observed, substantiating their importance in hydrolysis, fermentation and acetogenesis processes in acclimatization and steady phases (Phases 1, 3 and 5). *Methanothrix* and related *Methanosaeta* strains were dominated at the beginning of Phase 3 (OLR 4 kg-COD/m³/d) and were gradually replaced by *Methanolinea* and *Methanospirillum* in Phase 5 (OLR 6 kg-COD/m³/d). This indicates the gradual transformation of the HBSAnMBR process from acetoclastic methanogenesis to hydrogenotrophic methanogenesis at high OLRs. The shift towards hydrogenotrophic methanogenesis can also be influenced by the increased presence of syntrophic bacteria that break down longer-chain fatty acids and alcohols, producing hydrogen and carbon dioxide as by-products

[85]. These by-products are then used by hydrogenotrophic methanogens for methane production [86]. Understanding these shifts is crucial for optimizing operational parameters to enhance the efficiency and stability of the methanogenesis process in an HBSAnMBR system.

In summary, the in-depth exploration of microbial dynamics and metabolic pathways in HBSAnMBR operation offers insights into the complex relationships governing the production of volatile fatty acids (VFAs) and biomethane. The identified microbes during the acclimatization phase (Phase 1), such as *Pseudomonas, Bacillus, Citrobacter, Klebsiella, Clostridia, Lactococcus,* and *Acinetobacter*, emerge as key players influencing VFA production and, consequently, impacting the overall performance of HBSAnMBR system. This study also unravels the importance of syntrophic bacteria, particularly *Anaerolineaceae* and *Candidatus Cloacimonas*, in cooperation with methanogens and the metabolic flexibility of *Methanothrix* for potentially utilizing the carbon dioxide reduction pathway for biomethane production. This process may yield more energy than acetate decarboxylation. The transition from acetoclastic to hydrogenotrophic methanogenesis during stable phases (Phases 3 – 6) at high OLRs underlines the adaptability of the SAnMBR system over prolonged and sustained operation. The inferences drawn from this comprehensive microbiological investigation can contribute to developing an efficient full-scale HBSAnMBR system to achieve high-rate treatment and subsequent biomethane production. The findings of this study can potentially be implemented for sustained operating conditions, ultimately leading to higher biomethane recovery and operational performance of the SAnMBR system.

4. Conclusion

A high-biomass submerged AnMBR (HBSAnMBR) treating abattoir wastewater was operated in 6 distinct phases at OLR 1.05 – 7 kg-COD/m³/d. During the most sustainable phase (Phase 3, OLR 4 kg-COD/m³/d), the HBSAnMBR demonstrated the highest biomethane recovery (75.5 $\pm$ 2.0%) and COD removal efficiency (98.8 $\pm$ 0.71%). The comprehensive whole genome sequencing and bioinformatics analysis indicate the distinct role and adaptation of specific microbial communities, particularly *Anaerolineaceae*, *P. extremaustralis*, and *Candidatus Cloacimonas*, under varying operational phases. This insight enhances our understanding of microbial resilience and functional diversity in high-organic-load environments. Furthermore, the detailed analysis of the transition from acetoclastic to hydrogenotrophic methanogenesis, driven by shifts in organic loading rates, offers a new perspective on microbial response and system efficiency in HBSAnMBR systems. Moreover, the integration of functional metagenomics analysis elucidates the complex metabolic pathways of *Anaerolineaceae* and *Pseudomonas* resulting in high VFA concentrations and biomethane recovery. Furthermore, it was observed that the methanogens, namely *Methanothrix* and *Methanosaeta,* utilized acetate to undergo acetoclastic methanogenesis at the beginning of the steady phase (Phase 1) at OLR 4 kg-COD/m³/d; however, replaced by hydrogenotrophic methanogenesis due to the metabolism of *Methanolinea* and *Methanospirillum* by the end of Phase 5 (OLR 6 kg-COD/m³/d) by utilizing propionate.

The outcomes of this study not only contribute to the academic understanding of microbial dynamics in abattoir wastewater treatment but also hold practical implications for the optimization and design of full-scale HBSAnMBR systems. Future research should focus on advancing real-time monitoring and adaptive management strategies in HBSAnMBR systems, tailoring them to the dynamic microbial responses for enhanced wastewater treatment efficiency and sustainability.

CRediT authorship contribution statement

Nuwan Vithanage: Writing – review & editing, Writing – original draft, Visualization, Validation, Software, Methodology, Investigation, Data curation. **Rajneesh Kumar Gautam:** Writing – review & editing, Writing – original draft, Visualization, Validation, Software, Methodology, Investigation, Formal analysis, Data curation, Conceptualization. **Dimuth Navaratna:** Writing – review & editing, Writing – original draft, Visualization, Validation, Supervision, Resources, Project administration, Methodology, Investigation, Conceptualization. **Shobha Muthukumaran:** Writing – review & editing, Writing – original draft, Supervision. **Nandkishor More:** Writing – review & editing, Supervision.

Declaration of Competing Interest

The authors declare that they have no known competing financial interests or personal relationships that could have appeared to influence the work reported in this paper.

Data availability

Data will be made available on request.

Acknowledgements

Appendix A. Supporting information

Supplementary data associated with this article can be found in the online version at doi:10.1016/j.bej.2024.109275.

References

[1] P.W. Harris, B.K. McCabe, Process optimisation of anaerobic digestion treating high-strength wastewater in the Australian red meat processing industry, Appl. Sci. 10 (21) (2020) 7947.

[2] J. Ananda, et al., Analysing behavioural and socio-demographic factors and practices influencing Australian household food waste, J. Clean. Prod. 306 (2021) 127280.

[3] B.R. Baker, et al., Advanced technologies for poultry slaughterhouse wastewater treatment: a systematic review, J. Dispers. Sci. Technol. 42 (6) (2021) 880–899.

[4] P.W. Harris, B.K. McCabe, Review of pre-treatments used in anaerobic digestion and their potential application in high-fat cattle slaughterhouse wastewater, Appl. Energy 155 (2015) 560–575.

[5] Z. Lei, et al., Characterization of microbial evolution in high-solids methanogenic co-digestion of canned coffee processing wastewater and waste activated sludge by an anaerobic membrane bioreactor, J. Clean. Prod. 232 (2019) 1442–1451.

[6] D. Kudisi, et al., Long-term performance, membrane fouling behaviors and microbial community in a hollow fiber anaerobic membrane bioreactor (HF-AnMBR) treating synthetic terephthalic acid-containing wastewater, J. Hazard. Mater. 424 (2022) 127458.

[7] S. Saha, et al., An integrated leachate bed reactor – anaerobic membrane bioreactor system (LBR-AnMBR) for food waste stabilization and biogas recovery, Chemosphere 311 (2023) 137054.

[8] P. Puengrang, et al., Diverse microbial community profiles of propionate-degrading cultures derived from different sludge sources of anaerobic wastewater treatment plants, Microorganisms 8 (2) (2020).

[9] S.N.F. Moideen, et al., Performance evaluation and energy potential analysis of anaerobic membrane bioreactor (AnMBR) in the treatment of simulated milk wastewater, Chemosphere 317 (2023) 137923.

[10] Y. Hu, et al., Recent developments of anaerobic membrane bioreactors for municipal wastewater treatment and bioenergy recovery: focusing on novel configurations and energy balance analysis, J. Clean. Prod. 356 (2022) 131856.

[11] Y. Wang, et al., Bioelectrochemical anaerobic membrane bioreactor enables high methane production from methanolic wastewater: roles of microbial ecology and microstructural integrity of anaerobic biomass, Chemosphere 339 (2023) 139676.

[12] M. Matsubayashi, et al., Phylogenetic diversity and in situ detection of eukaryotes in anaerobic sludge digesters, PLoS One 12 (3) (2017) e0172888.

[13] S.I. Padmasiri, et al., Methanogenic population dynamics and performance of an anaerobic membrane bioreactor (AnMBR) treating swine manure under high shear conditions, Water Res. 41 (1) (2007) 134–144.

[14] A. Saravanan, et al., Strategies for enhancing the efficacy of anaerobic digestion of food industry wastewater: an insight into bioreactor types, challenges, and future scope, Chemosphere 310 (2023) 136856.

[15] Khan, M.A., Optimization and Performance Improvement of Anaerobic Membrane Biocreactor (AnMBR) for Volatile Fatty Acid and Biohydrogen Production. 2019.

[16] S.M.A. Abuabdou, et al., A review of anaerobic membrane bioreactors (AnMBR) for the treatment of highly contaminated landfill leachate and biogas production: effectiveness, limitations and future perspectives, J. Clean. Prod. 255 (2020) 120215.

[17] T.-S. Le, et al., Two-stage anaerobic membrane bioreactor for co-treatment of food waste and kitchen wastewater for biogas production and nutrients recovery, Chemosphere 309 (2022) 136537.

[18] A.D. Grossman, et al., Effect of ultrafiltration membrane material on fouling dynamics in a submerged anaerobic membrane bioreactor treating domestic wastewater, Environ. Sci. Water Res. Technol. 5 (6) (2019) 1145–1156.

[19] J. Ji, et al., Submerged anaerobic membrane bioreactor applied for mainstream municipal wastewater treatment at a low temperature: sludge yield, energy balance and membrane filtration behaviors, J. Clean. Prod. 355 (2022) 131831.

[20] G. Balcıoğlu, G. Yilmaz, Z.B. Gönder, Evaluation of anaerobic membrane bioreactor (AnMBR) treating confectionery wastewater at long-term operation under different organic loading rates: performance and membrane fouling, Chem. Eng. J. 404 (2021) 126261.

[21] N. Basset, et al., Start-up and operation of an AnMBR for winery wastewater treatment, Ecol. Eng. 86 (2016) 279–289.

[22] T. Wang, et al., In-depth insights into the temporal-based fouling mechanism and its exploration in anaerobic membrane bioreactors: a review, J. Clean. Prod. 375 (2022) 134110.

[23] A. Olubukola, et al., Development of a dynamic model for effective mitigation of membrane fouling through biogas sparging in submerged anaerobic membrane bioreactors (SAnMBRs), J. Environ. Manag. 323 (2022) 116151.

[24] P. Jensen, et al., Anaerobic membrane bioreactors enable high rate treatment of slaughterhouse wastewater, Biochem. Eng. J. 97 (2015) 132–141.

[25] H. Cheng, et al., Bioenergy recovery from methanogenic co-digestion of food waste and sewage sludge by a high-solid anaerobic membrane bioreactor (AnMBR): mass balance and energy potential, Bioresour. Technol. 326 (2021) 124754.

[26] R.K. Gautam, et al., Evaluation of long-term operational and treatment performance of a high-biomass submerged anaerobic membrane bioreactor treating abattoir wastewater, Chem. Eng. J. (2023) 142145.

[27] S. Keskes, et al., Performance of a submerged membrane bioreactor for the aerobic treatment of abattoir wastewater, Bioresour. Technol. 103 (1) (2012) 28–34.

[28] D. Navaratna, V. Jegatheesan, Implications of short and long term critical flux experiments for laboratory-scale MBR operations, Bioresour. Technol. 102 (9) (2011) 5361–5369.

[29] W.E. Federation, A. Association, Standard methods for the examination of water and wastewater. American Public Health Association (APHA), Washington, DC, USA,, 2005.

[30] K.F. Oakeson, et al., Bioinformatic analyses of whole-genome sequence data in a public health laboratory, Emerg. Infect. Dis. 23 (9) (2017) 1441–1445.

[31] D. Wu, et al., Effect of Fenton-like reactions on the hydrolysis efficiency of lignocellulose during rice straw composting based on genomics and metabolomics sequencing, J. Clean. Prod. 396 (2023) 136493.

[32] K. Chau, et al., Evaluation of metagenomic, 16S rRNA gene and ultra-plexed PCR-based sequencing approaches for profiling antimicrobial resistance gene and bacterial taxonomic composition of polymicrobial samples, bioRxiv (2022), 2022.05.12.491637.

[33] M. Kanehisa, S. Goto, KEGG: Kyoto encyclopedia of genes and genomes, Nucleic Acids Res. 28 (1) (2000) 27–30.

[34] H. Zhang, et al., Modeling the Methane Production Kinetics of Anaerobic Co-Digestion of Agricultural Wastes Using Sigmoidal Functions, Energies 14 (2) (2021) 258.

[35] R.K. Gautam, et al., Recovery of biomethane from a submerged anaerobic membrane bioreactor treating domestic wastewater blended with semi-solid organic wastes discharged from residential establishments, Environ. Technol. Innov. 27 (2022) 102763.

[36] M.H. Zwietering, et al., Modeling of the bacterial growth curve, Appl. Environ. Microbiol. 56 (6) (1990) 1875–1881.

[37] S. Verma, et al., Sampling typology and techniques, Int. J. Sci. Res. Dev. 5 (9) (2017) 298–301.

[38] M. Peleg, M.G. Corradini, Microbial growth curves: what the models tell us and what they cannot, Crit. Rev. Food Sci. Nutr. 51 (10) (2011) 917–945.

[39] Q. Yu, L. Feng, X. Zhen, Effects of organic loading rate and temperature fluctuation on the microbial community and performance of anaerobic digestion of food waste, Environ. Sci. Pollut. Res. Int. 28 (11) (2021) 13176–13187.

[40] T.-D.-H. Vo, et al., Influence of organic loading rates on treatment performance of membrane bioreactor treating tannery wastewater, Environ. Technol. Innov. 24 (2021) 101810.

[41] C. Juntawang, C. Rongsayamanont, E. Khan, Entrapped cells-based-anaerobic membrane bioreactor treating domestic wastewater: performances, fouling, and bacterial community structure, Chemosphere 187 (2017) 147–155.

[42] N. Guo, et al., Effects of the food-to-microorganism (F/M) ratio on N2O emissions in aerobic granular sludge sequencing batch airlift reactors, Water 9 (7) (2017) 477.

[43] R.A. Hamza, et al., Impact of food-to-microorganisms ratio on the stability of aerobic granular sludge treating high-strength organic wastewater, Water Res 147 (2018) 287–298.

[44] M.H. Zwietering, et al., Modeling of the bacterial growth curve, Appl. Environ. Microbiol. 56 (6) (1990) 1875–1881.

[45] M. Atasoy, O. Eyice, Z. Cetecioglu, A comprehensive study of volatile fatty acids production from batch reactor to anaerobic sequencing batch reactor by using cheese processing wastewater, Bioresour. Technol. 311 (2020) 123529.

[46] H. Cheng, et al., Enhancement of sustainable flux by optimizing filtration mode of a high-solid anaerobic membrane bioreactor during long-term continuous treatment of food waste, Water Res. 168 (2020) 115195.

[47] D.M. Yin, et al., Volatile fatty acids (VFA) production and recovery from chicken manure using a high-solid anaerobic membrane bioreactor (AnMBR), Membranes 12 (11) (2022) 1133.

[48] Y. Sharma, B. Li, Optimizing energy harvest in wastewater treatment by combining anaerobic hydrogen producing biofermentor (HPB) and microbial fuel cell (MFC), Int. J. Hydrog. Energy 35 (8) (2010) 3789–3797.

[49] A.J. Cavaleiro, et al., Continuous high rate anaerobic treatment of oleic acid based wastewater is possible after a step feeding start-up, Environ. Sci. Technol. 43 (8) (2009) 2931–2936.

[50] Y.W. Berkessa, et al., Novel anaerobic membrane bioreactor (AnMBR) design for wastewater treatment at long HRT and high solid concentration, Bioresour. Technol. 250 (2018) 281–289.

[51] T. Inaba, et al., Microbial community in an anaerobic membrane bioreactor and its performance in treating organic solid waste under controlled and deteriorated conditions, J. Environ. Manag. 269 (2020) 110786.

[52] Q. Dong, W. Parker, M. Dagnew, Long term performance of membranes in an anaerobic membrane bioreactor treating municipal wastewater, Chemosphere 144 (2016) 249–256.

[53] M. Atasoy, et al., Bio-based volatile fatty acid production and recovery from waste streams: current status and future challenges, Bioresour. Technol. 268 (2018) 773–786.

[54] A. Sepehri, M.-H. Sarrafzadeh, Effect of nitrifiers community on fouling mitigation and nitrification efficiency in a membrane bioreactor, Chem. Eng. Process. - Process. Intensif. 128 (2018) 10–18.

[55] L.-J. Wu, et al., High loading anaerobic co-digestion of food waste and grease trap waste: determination of the limit and lipid/long chain fatty acid conversion, Chem. Eng. J. 338 (2018) 422–431.

[56] S. Wainaina, et al., Bioengineering of anaerobic digestion for volatile fatty acids, hydrogen or methane production: a critical review, Bioengineered 10 (1) (2019) 437–458.

[57] V. Patel, S. Pandit, K. Chandrasekhar, Basics of methanogenesis in anaerobic digester, in: V.C. Kalia (Ed.), in Microbial Applications Vol.2: Biomedicine, Agriculture and Industry, Springer International Publishing, Cham, 2017, pp. 291–314.

[58] R. Loganath, J. Senophiyah-Mary, Critical review on the necessity of bioelectricity generation from slaughterhouse industry waste and wastewater using different anaerobic digestion reactors, Renew. Sustain. Energy Rev. 134 (2020) 110360.

[59] G. Demirer, S. Chen, Effect of retention time and organic loading rate on anaerobic acidification and biogasification of dairy manure, J. Chem. Technol. Biotechnol. 79 (12) (2004) 1381–1387.

[60] Y. Hu, et al., A review on anaerobic membrane bioreactors for enhanced valorization of urban organic wastes: achievements, limitations, energy balance and future perspectives, Sci. Total Environ. 820 (2022) 153284.

[61] A. Sepehri, M.-H. Sarrafzadeh, Activity enhancement of ammonia-oxidizing bacteria and nitrite-oxidizing bacteria in activated sludge process: metabolite reduction and CO2 mitigation intensification process, Appl. Water Sci. 9 (5) (2019) 131.

[62] K.C. Wijekoon, C. Visvanathan, A. Abeynayaka, Effect of organic loading rate on VFA production, organic matter removal and microbial activity of a two-stage thermophilic anaerobic membrane bioreactor, Bioresour. Technol. 102 (9) (2011) 5353–5360.

[63] L. Metcalf, H.P. Eddy, G. Tchobanoglous. Wastewater Engineering: Treatment, Disposal, and Reuse Vol. 4, McGraw-Hill, New York, 1991.

[64] J.B. Holm-Nielsen, T. Al Seadi, P. Oleskowicz-Popiel, The future of anaerobic digestion and biogas utilization, Bioresour. Technol. 100 (22) (2009) 5478–5484.

[65] G. Płaza, et al., Insights into the microbial diversity and structure in a full-scale municipal wastewater treatment plant with particular regard to Archaea, PLOS ONE 16 (4) (2021) e0250514.

[66] M. Balat, H. Balat, Biogas as a renewable energy source—a review, Energy Sources, Part A 31 (14) (2009) 1280–1293.

[67] S. Isazadeh, S. Jauffur, D. Frigon, Bacterial community assembly in activated sludge: mapping beta diversity across environmental variables, Microbiologyopen 5 (6) (2016) 1050–1060.

[68] A.L. Smith, et al., Perspectives on anaerobic membrane bioreactor treatment of domestic wastewater: a critical review, Bioresour. Technol. 122 (2012) 149–159.

[69] R. Conrad, Microbial ecology of methanogens and methanotrophs, Adv. Agron. 96 (2007) 1–63.

[70] P.M. Tribelli, et al., Microaerophilic alkane degradation in Pseudomonas extremaustralis: a transcriptomic and physiological approach, J. Ind. Microbiol. Biotechnol. 45 (1) (2018) 15–23.

[71] J. Guo, et al., Dissecting microbial community structure and methane-producing pathways of a full-scale anaerobic reactor digesting activated sludge from wastewater treatment by metagenomic sequencing, Microb. Cell Fact. 14 (2015) 33.

[72] B. Liang, et al., Anaerolineaceae and Methanosaeta turned to be the dominant microorganisms in alkanes-dependent methanogenic culture after long-term of incubation, AMB Express 5 (1) (2015) 117.

[73] W. Zhai, et al., Abundance and diversity of microbial arsenic biotransformation genes in the sludge of full-scale anaerobic digesters from a municipal wastewater treatment plant, Environ. Int. 138 (2020) 105535.

[74] L.A. Johnson, L.A. Hug, Cloacimonadota metabolisms include adaptations for engineered environments that are reflected in the evolutionary history of the phylum, bioRxiv (2021), 2021.10.08.463351.

[75] V. Bhandari, R.S. Gupta, The phylum Thermotogae, in: in: The Prokaryotes: Other Major Lineages of Bacteria and The Archaea, Springer Berlin Heidelberg, Berlin, Heidelberg, 2014, pp. 989–1015.

[76] E. Evans, M.R. Brown, P. Gilbert, Iron chelator, exopolysaccharide and protease production in Staphylococcus epidermidis: a comparative study of the effects of specific growth rate in biofilm and planktonic culture, Microbiology 140 (1994) 153–157.

[77] N.R. Buan, Methanogens: pushing the boundaries of biology, Emerg. Top. Life Sci. 2 (4) (2018) 629–646.

[78] B.A. Huser, K. Wuhrmann, A.J.B. Zehnder, Methanothrix soehngenii gen. nov. sp. nov., a new acetotrophic non-hydrogen-oxidizing methane bacterium, Arch. Microbiol. 132 (1) (1982) 1–9.

[79] I. Sánchez-Andrea, et al., The reductive glycine pathway allows autotrophic growth of Desulfovibrio desulfuricans, Nat. Commun. 11 (1) (2020) 5090.

[80] Y. Zhang, et al., Syntrophy mechanism, microbial population, and process optimization for volatile fatty acids metabolism in anaerobic digestion, Chem. Eng. J. 452 (2023) 139137.

[81] X. Zhu, et al., Metabolic dependencies govern microbial syntrophies during methanogenesis in an anaerobic digestion ecosystem, Microbiome 8 (1) (2020) 22.

[82] B. Liang, et al., High Frequency of Thermodesulfovibrio spp. and Anaerolineaceae in Association with Methanoculleus spp. in a Long-Term Incubation of n-Alkanes-Degrading Methanogenic Enrichment Culture, Front. Microbiol. 7 (2016).

[83] R. Mei, et al., Metagenomic and metatranscriptomic analyses revealed uncultured bacteroidales populations as the dominant proteolytic amino acid degraders in anaerobic digesters, Front. Microbiol. 11 (2020) 593006.

[84] P. Yang, et al., Metatranscriptomic evidence for classical and RuBisCO-mediated CO2 reduction to methane facilitated by direct interspecies electron transfer in a methanogenic system, Sci. Rep. 9 (1) (2019) 4116.

[85] M.B. Kurade, et al., Acetoclastic methanogenesis led by Methanosarcina in anaerobic co-digestion of fats, oil and grease for enhanced production of methane, Bioresour. Technol. 272 (2019) 351–359.

[86] M. Westerholm, M. Calusinska, J. Dolfing, Syntrophic propionate-oxidizing bacteria in methanogenic systems, FEMS Microbiol. Rev. 46 (2) (2022).